ELSEVIER

Biophysical Chemistry 53 (1995) 213–218

Biophysical Chemistry

# Bistability and reaction thresholds in the phenol-inhibited peroxidase-catalyzed oxidation of indole-3-acetic acid

S.N. Krylov [a], B.D. Aguda [a,*], M.L. Ljubimova [b]

[a] Department of Chemistry and Biochemistry, Laurentian University, Sudbury, Ontario, Canada P3E 2C6
[b] Institute for Nuclear Physics, Moscow State University, Moscow 119899, Russian Federation

Received 14 March 1994; accepted in revised form 9 August 1994

## Abstract

A model mechanism for the phenol-inhibited peroxidase-catalyzed oxidation of indole-3-acetic acid (IAA) is proposed and analyzed. The model involves an autocatalytic free radical species that sustains IAA oxidation and the phenolic inhibitor acting as a free radical scavenger. Under a fixed set of parameter values, the model exhibits a coexistence of two stable steady states. This bistability phenomenon explains the origin of the experimentally observed threshold inhibitor concentrations above which IAA oxidation stops. The variation of the inhibitor threshold level with enzyme and substrate concentrations are reproduced by the model almost quantitatively.

*Keywords:* Oxidation of indole-3-acetic acid; Phenol inhibition mechanism; Reaction threshold; Bistability; Modelling; Computer simulation

## 1. Introduction

Indole-3-acetic acid (IAA) is a natural phytohormone with many growth regulatory functions. The concentration level of IAA in plants depends, in particular, on the rate of its oxidation which is catalyzed by IAA-oxidases, many of which are peroxidases. The rate of the peroxidase-catalyzed oxidation of IAA is affected by natural phenolic inhibitors such as caffeic acid, gallic acid, chlorogenic acid, and others.

In this paper, we propose a model mechanism of phenol inhibition to explain the experimental observations reported earlier [1,2]. Previous investigators [3–8] have suggested that phenols inhibit the peroxidase-catalyzed oxidation of IAA by acting as competing substrates for the enzyme. Reported Lineweaver–Burk plots [5,9], however, are inconsistent with a competitive inhibition mechanism. Our proposed model suggests that phenols inhibit IAA oxidation by scavenging the free radicals that drive the peroxidase-catalyzed reaction.

It was found in previous experiments [1] that, under some conditions, a well-defined level of inhibitor concentration exists above which IAA oxidation stops. Below this threshold inhibitor concentration, the oxidation rate is almost unaffected. Analysis of our model mechanism provides a clear explanation of the origin of this threshold concentration. The model exhibits a coexistence of two stable steady states, one of which corresponds to the inhibited reaction while the other corresponds to the un-in-

---

[*] Corresponding author.

*SSDI* 0301-4622(94)00106-5

hibited reaction. The boundary that separates the stability regions of these two steady states defines the threshold inhibitor concentration.

We first give a summary of the relevant experimental observations in Section 2. In Section 3, the proposed model mechanism is described and a discussion is given on the choice of appropriate parameter values. Analysis of the model and computer simulations are presented in Section 4.

## 2. Summary of relevant experimental results

Details of our experiments demonstrating the existence of inhibitor threshold concentrations have been reported previously [1]. For the particular experiments described here, caffeic acid is the phenolic inhibitor and horseradish peroxidase is the enzyme catalyzing IAA oxidation. A summary is given below of the experimental observations that led us to propose a set of reaction steps for the model mechanism.

It was observed that further addition of the enzyme solution does not restart a previously inhibited reaction even if the enzyme concentration, [E], is greater than the inhibitor concentration, [I]. Likewise, dilution of the reaction mixture with the phosphate buffer (used to prepare our reagents) does not reinitiate IAA oxidation. Surprisingly, however, an inhibited reaction is reinitiated by the further addition of a solution of IAA. The inhibited reaction is also reinitiated by light irradiation in the presence of rose bengal, a photosensitizer; in this case, after reinitiation, the reaction proceeded without light and has the same kinetics as though it was not inhibited previously.

To measure the threshold inhibitor concentration, $I_{\mathrm{thr}}$, the chemiluminescence intensity during IAA oxidation was monitored for various inhibitor concentrations (see, for example, Fig. 1 of Ref. [1]). It is important to note that the variation of $I_{\mathrm{thr}}$ as a function of substrate or enzyme concentration depends on the relative order in which the inhibitor and enzyme are added to the reaction mixture.

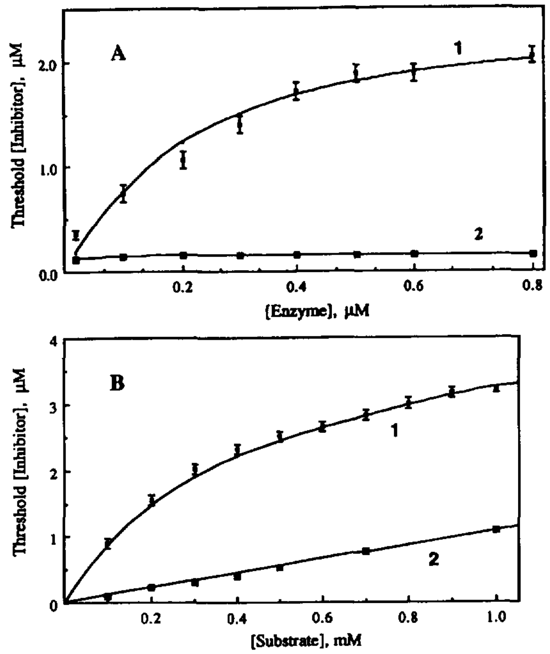

Fig. 1. (A) Threshold inhibitor concentration as a function of enzyme concentration for fixed substrate concentration. (B) Threshold inhibitor concentration as a function of substrate concentration for fixed enzyme concentration. For both (A) and (B), the experimental data points near curve 1 correspond to the case when the enzyme is added to the reaction mixture before the inhibitor; data points near curve 2 correspond to the case when the inhibitor is added before the enzyme. See Ref. [1] for details of the experiments. Note that curves 1 and 2 for both (A) and (B) correspond to the bifurcation points of the steady-state diagrams (e.g. values of $[\mathrm{I}]_0$ corresponding to the right and left 'knees', respectively, of Fig. 3).

The variation of $I_{\mathrm{thr}}$ as a function of [E] (for fixed substrate concentration, [S]) is shown in Fig. 1A. Here, the experimental points near curve 1 correspond to the case where the enzyme is added to the reaction mixture *before* the inhibitor. $I_{\mathrm{thr}}$ initially increases with increasing [E] and then levels off. Experimental points near curve 2 correspond to the case where the enzyme is added *after* the inhibitor; in this case, $I_{\mathrm{thr}}$ is independent of [E].

The dependence of $I_{\mathrm{thr}}$ as a function of the substrate concentration [S] (for fixed [E]) is shown in Fig. 1B. Experimental points near curve 1 correspond to the case where E was added before I. Points near curve 2 show the dependence for the case where E is added after I; here, $I_{\mathrm{thr}}$ is directly proportional to [S]. It was also observed that if E is added before I, then $I_{\mathrm{thr}}$ depends on the time of addition of I. Curves 1 and 2 in both Fig. 1A and 1B are generated by the model mechanism that we discuss next.

## 3. Model mechanism

### 3.1. Reaction steps

Our main postulate is that the inhibitor I depletes a free radical species R which drives the oxidation of the substrate. Traces of R must be found in the substrate solution because of the fact that the inhibited reaction can be reinitiated by the addition of more substrate solution. Besides being produced spontaneously from the substrate S, R is also autocatalytically produced in the peroxidase-catalyzed substrate oxidation. The phenolic inhibitor is a scavenger of R, a claim that is supported by the fact that the effect of anphen (a free radical scavenger) on the peroxidase-catalyzed IAA oxidation is similar to that of phenolic inhibitors. The reaction steps in our model are the following:

$$S \xrightarrow{k_1} R, \qquad (R1)$$

$$S + R + E \underset{k_2^{(3)}}{\overset{k_1^{(1)}}{\rightleftharpoons}} ERS \xrightarrow{k_2^{(2)}} E + 2R, \qquad (R2)$$

$$R + R \xrightarrow{k_3} P_1, \qquad (R3)$$

$$R + I \xrightarrow{k_4} I^{\cdot} + P_2, \qquad (R4)$$

$$I^{\cdot} \xrightarrow{k_5} I, \qquad (R5)$$

$$I^{\cdot} + I^{\cdot} \xrightarrow{k_6} P_3, \qquad (R6)$$

where S is the substrate (IAA), R is a free radical, E is the free enzyme, ERS is an enzyme–substrate–free radical complex, I is the phenolic inhibitor, $I^{\cdot}$ is a free radical derived from the inhibitor, and $P_1$, $P_2$, $P_3$ are some end products of the reaction (these are not involved in the dynamical equations discussed below). A network diagram is provided in Fig. 2 to show the structure of the mechanism.

Reaction (R1) represents the spontaneous generation of the free radical R from the substrate. (R2) summarizes the enzyme-catalyzed reaction steps in which R is produced autocatalytically. The formation of the ERS complex is essential for the explanation of the experimental results. Reaction (R3) assumes a second order termination of R into some inert products (this reaction could be a dimerization or disproportionation reaction). Reaction (R4) represents the reaction between the free radical R and the inhibitor to form the free radical $I^{\cdot}$; this reaction is the direct cause of the inhibition of the IAA oxidation reaction. Reaction (R5) is the reduction of the free radical $I^{\cdot}$ to I (the electron donor is not shown in the reaction). The last reaction step, (R6), is a termination reaction for the free radical $I^{\cdot}$. The model would explain the inhibition as follows: if $I > I_{\text{thr}}$, reaction (R4) is faster than the autocatalytic reaction (R2) and IAA oxidation is inhibited; if $I < I_{\text{thr}}$, then the reverse is true.

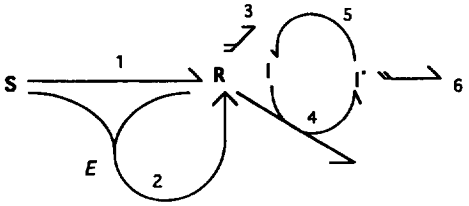

$k_1 = 10^{-9}\ \text{s}^{-1}$

$k_2^{(2)} = 0.017\ \text{s}^{-1}$

$k_3 = 2.7 \times 10^7\ \text{M}^{-1}\text{s}^{-1}$

$k_4 = 10^7\ \text{M}^{-1}\text{s}^{-1}$

$k_5 = 10^{-6}\ \text{s}^{-1}$

$K_m = 9.3 \times 10^{-12}\ \text{M}^2$

Fig. 2. Network diagram of the model corresponding to reactions (R1) to (R6) in the text. The set of parameter values given are those that give optimal fit to the experimental data points given in Fig. 1.

### 3.2. Dynamical equations

In the time scale of the dynamics of R, I, and $I^{\cdot}$, the concentration of the substrate, [S], is assumed to be constant at a value of $S_0$. Our experimental conditions are such that $[E] \ll [S]$ and $[R] \ll [S]$. From the enzyme conservation condition, we have $[E] + [ERS] = E_0$ where $E_0$ is the initial concentration of the enzyme. It is also assumed that the enzyme species E and ERS attain their steady state levels rapidly. Note that reaction (R3) involves a free-radical recombination; in addition to R, the complexed free-radical ERS can also undergo reactions similar to (R3), i.e. ERS + ERS → products, or R + ERS → products. Furthermore, ERS can also undergo a reaction similar to (R4), i.e. ERS + I → $I^{\cdot}$

+ products. To include all these possibilities, let $[\mathrm{R}]+[\mathrm{ERS}]=R_0(t)$ and from now on substitute $R_0$ in reactions (R3) and (R4) instead of just $R$. From these assumptions, the following expression is obtained:

$$[\mathrm{ERS}]=\frac{\beta-\sqrt{\beta^2-4S_0^2E_0R_0}}{2S_0}, \tag{1}$$

where $\beta=K_m+(R_0+E_0)S_0$ and $K_m$ is the Michaelis–Menten constant defined as

$$K_m=\frac{k_2^{(2)}+k_2^{(3)}}{k_2^{(1)}}.$$

Using the expression for [ERS] given in Eq. (1) and ignoring reaction (R6) which is insignificant for low $\mathrm{I}^{\cdot}$ levels, the dynamical equations are the following:

$$\frac{\mathrm{d}R_0}{\mathrm{d}t}=k_1S_0+k_2^{(2)}[\mathrm{ERS}]-k_3R_0^2-k_4R_0I, \tag{2a}$$

$$\frac{\mathrm{d}I}{\mathrm{d}t}=-k_4R_0I+k_5(I_0-I), \tag{2b}$$

where $I_0$ is the initial inhibitor concentration and [ERS] is given by Eq. (1). Note that $I^{\cdot}=I_0-I$ was used in the second term on the right-hand side of equation (2b). Also, any constant factor preceding the term $k_3R_0^2$ in Eq. (2a) is absorbed in the constant $k_3$.

### 3.3. Model parameters

The parameter values used in the computer simulations are based on various experimental observations. Rate coefficient $k_1$ was estimated as follows: first, note that when the enzyme is added to the mixture of substrate and inhibitor, and the inhibitor concentration is slightly higher than the threshold concentration, $I_{\mathrm{thr}}$, there is a measurable lag period prior to the start of the reaction [2]. After this lag period, the amount of I that is consumed is approximately equal to $(I_0-I_{\mathrm{thr}})$ where $I_0$ is the initial concentration of the inhibitor. Thus, a reasonable estimate of the rate of production, $v$, of species $R$ is $v=(I_0-I_{\mathrm{thr}})/(\text{lag period})$. Experiments performed to determine the effect of the period of incubation (i.e. from the time S and I are mixed until E is added) on the lag period showed that, within a precision of 10%, the lag period is unaffected. Our experiments give a typical value of $v$ of $10^{-11}$ M $\mathrm{s}^{-1}$. It is assumed that the production of R during the incubation time is due to reaction (R1) which has a rate of $v_1\leqslant 0.1\,v$. We have $v_1=\mathrm{d}R/\mathrm{d}t=k_1S$, so $k_1=v_1/S\leqslant 0.1\,v/S$. A typical value of $S$ is $10^{-3}$ M, hence $k_1\leqslant 1\times10^{-9}\ \mathrm{s}^{-1}$.

When I was added before E to the reaction mixture, we have $\mathrm{R}\ll\mathrm{E}$ and $\mathrm{R}\ll\mathrm{S}$ and the following steady state concentration of the ERS complex can be derived:

$$[\mathrm{ERS}]_{\mathrm{ss}}=\frac{E_0R_0S_0}{K_m+E_0S_0}. \tag{3}$$

The steady state condition for $R_0$ is then

$$\frac{\mathrm{d}R_0}{\mathrm{d}t}=k_1S_0+k_2^{(2)}\frac{E_0R_0S_0}{K_m+E_0S_0}-k_3R_0^2-\frac{k_4k_5R_0I_0}{k_4R_0+k_5}=0. \tag{4}$$

Since $R_0$ is very small, the term $(-k_3R_0^2)$ can be neglected and the roots of the following polynomial give the steady state values of $R_0$:

$$k_2k_4R_0^2+(k_4k_1S_0+k_2k_5-k_4k_5I_0)R_0+k_5k_1S_0=0, \tag{5}$$

where

$$k_2=k_2^{(2)}\frac{E_0S_0}{K_m+E_0S_0}. \tag{6}$$

Eq. (5) is a quadratic equation in $R_0$ with two positive roots if $I_0$ is greater than some value $I^*$. At $I_0=I^*$ the two roots coalesce and we only have one steady state value for $R_0$. It turns out that $I^*$ corresponds to the experimentally measured $I_{\mathrm{thr}}$. Solving for $I^*$ gives

$$I^*=\frac{k_1S_0}{k_5}+\frac{k_2}{k_4}+2\sqrt{\frac{k_2}{k_4}\frac{k_1S_0}{k_5}}. \tag{7}$$

Experimentally, $I_{\mathrm{thr}}$ is directly proportional to $S_0$ (see curve 2 of Fig. 1B) which implies, from Eq. (7), that

$$\frac{k_1S_0}{k_5}\gg\frac{k_2}{k_4}. \tag{8}$$

Strictly, $I^*$ has a dependence on $E_0$ through the term involving $k_2$ (see Eq. (6) and (7)) but due to (8) we see that $I^*$ is independent of $E_0$. This agrees with our experimental observation that $I_{\text{thr}}$ does not depend on $E_0$ (see curve 2 of Fig. 1A).

From Eq. (6), the maximum value of $k_2$ is $k_2^{(2)}$ which is approached when $E_0 S_0 \gg K_m$. Thus, Eq. (8) can be rewritten as

$$\frac{k_1 S_0}{k_5} \gg \frac{k_2^{(2)}}{k_4}. \tag{9}$$

From curve 2 of Fig. 1B, the slope of the straight line is approximately equal to $k_1/k_5$ in our model. The value of the slope obtained from the experiment is $10^{-3}$. Using the estimate for $k_1$ ($\approx 10^{-9}$ s$^{-1}$), we obtain an estimate of $k_5 \approx 10^{-6}$ s$^{-1}$.

We set $k_4 = 10^7$ M$^{-1}$ s$^{-1}$ and, using a minimum value of $S_0$ (which is $10^{-4}$ M in our experiments), inequality (9) gives $k_2^{(2)} \ll 1$. It is found that a value of $k_2^{(2)} = 0.017$ s$^{-1}$ fits the experimental data very well. Our computer simulations gave an optimum value of $2.7 \times 10^7$ M$^{-1}$ s$^{-1}$ that fits the experimental data.

The value of $K_m$ is approximately equal to $E_0 S_0$, where $E_0$ corresponds to (maximum $I_{\text{thr}}$)/2 of curve 1 in Fig. 1A. This gave us an estimate of $K_m$ in the order of $10^{-11}$ M$^2$. Our computer simulations gave the optimum value of $9.3 \times 10^{-12}$ M$^2$.

The final set of parameters used in our computer simulations are listed below the network diagram in Fig. 2. Note that only those parameters needed in Eq. (2a) and (2b) are identified.

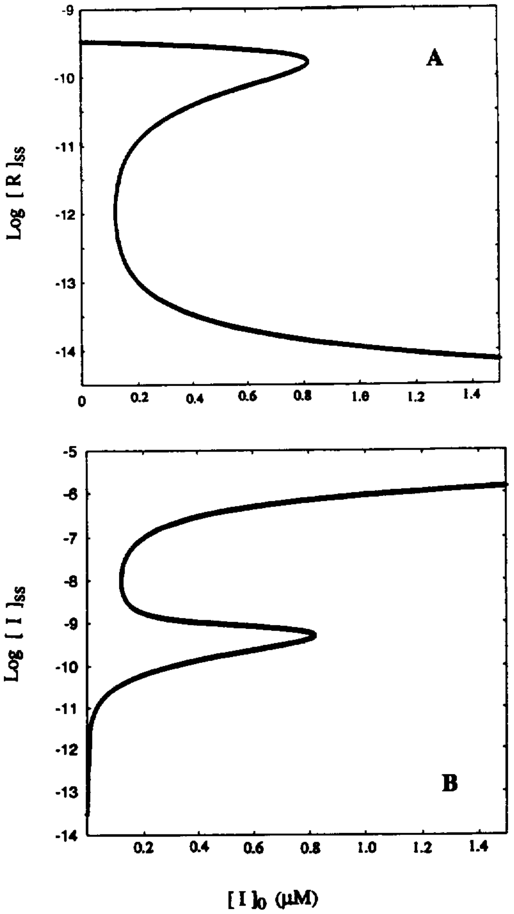

Fig. 3. (A) Steady state of R as a function of initial inhibitor concentration, $I_0$. (B) Steady state of I as a function of $I_0$. Both steady states, $R_{ss}$ and $I_{ss}$, are calculated from Eqs. (2a) and (2b) using the parameter values given in Fig. 2.

## 4. Analysis of the model and computer simulations

Graphs of the steady, $R_{ss}$ and $I_{ss}$, versus the initial concentration of the inhibitor, $I_0$, are shown in Fig. 3. There exists a range of $I_0$ values that gives rise to three steady states of R and I. Eq. (2b) indicates that

$$I_{ss} = \frac{k_5 I_0}{k_5 + k_4 R_{ss}} \tag{10}$$

Thus, the upper branch of the $R_{ss}$ curve in Fig. 3A corresponds to the lower branch of the $I_{ss}$ curve in Fig. 3B. Fig. 3B shows that if $I_0 < I_L$ (where $I_L \approx 0.1$ μM corresponding to the left 'knee' of the curve) then $I_{ss}$ is on the lower branch and, correspondingly, $R_{ss}$ is located on the upper branch. Thus, for $I_0 < I_L$, the reaction is not inhibited. Once $I_0 > I_L$, and if the inhibitor is added *before the enzyme*, then there are no R species to consume the added $I_0$ so that $I_{ss}$ is located on the upper branch and therefore $R_{ss}$ is now on the lower branch which means that the reaction is inhibited. Thus, when the inhibitor is added before the enzyme, $I_{\text{thr}} = I_L$. The value of $I_L$ is independent of [E] which explains the horizontal line (curve 2) in Fig. 1A.

When the inhibitor is added to the reaction mixture *after the enzyme*, depending on the time of addition of the inhibitor, the value of $I_{\mathrm{thr}}$ will be between $I_{\mathrm{L}}$ and $I_{\mathrm{R}}$ where $I_{\mathrm{R}} \approx 0.8$ μM corresponding to the right 'knee' of the steady state curve. The middle branch of the $I_{\mathrm{ss}}$ curve represents unstable steady states (called saddle points). The portrait of the dynamics on a phase plane (which has R and I as coordinates) has a separatrix that delineates those initial I concentrations leading to low $R_{\mathrm{ss}}$ (inhibited reaction) from those initial I concentrations that lead to high $R_{\mathrm{ss}}$ (reaction). Strictly speaking, it is this separatrix that determines the threshold inhibitor concentrations. It is now clear that the dependence of $I_{\mathrm{thr}}$ on the time of addition of the inhibitor to the reaction mixture is due to the time dependent concentration of R. We have arbitrarily considered the $I_0$ values corresponding to the right 'knee' ($I_{\mathrm{R}}$) of the steady state curves as the threshold inhibitor concentration when the enzyme is added before the inhibitor. These values of $I_{\mathrm{R}}$ are what we plotted in curve 1 for both Figs. 1A and 1B.

## 5. Concluding remarks

A model mechanism has been proposed for the inhibition of the peroxidase-catalyzed oxidation of IAA. This model is, of course, an abstraction of the complex detailed mechanism of this reaction which would involve enzymatic species such as compounds **I**, **II**, and **III**, as well as other various intermediates (see Ref. [10] for example).

Our model exhibits bistability which explains the origin of the experimentally-observed threshold inhibitor concentrations above which IAA oxidation is turned off. The phenomenon of bistability has been known for a long time in the peroxidase-oxidase reaction with reduced nicotinamide adenine dinucleotide (NADH) as substrate [11]; our results indicate that one can also observe bistability using IAA as substrate. This remains to be demonstrated in the laboratory.

## Acknowledgements

This work is partially supported by a research grant from the Natural Sciences and Engineering Research Council of Canada (to BDA) and a grant from the Special Foundation for Talented Young Scientists of Russia (to SNK).

## References

[1] S.N. Krylov, S.M. Krylova, and L.B. Rubin, Phytochemistry 33 (1993) 9.

[2] S.N. Krylov, S.M. Krylova, I.G. Chebotarev, and A.B. Chebotareva, Phytochemistry 36 (1994) 263.

[3] G.W. Schaeffer, J.G. Buta and F. Sharpe, Physiol. Plantarum 20 (1967) 342.

[4] T. Sonier, Y. Yoneda and F. Rodriguez-Tormes, Plant Physiol. 43 (1968) 1141.

[5] D.A. Gelinas, Plant Physiol. 51 (1973) 967.

[6] T.T. Lee, Plant Physiol. 59 (1977) 372.

[7] T.T. Lee, G.L. Rock and A. Stoessl, Phytochemistry 17 (1978) 1721.

[8] W.A. Andreae, Nature 170 (1952) 83.

[9] N.F. Haard, Z. Pflanzenphysiol. 89 (1978) 87.

[10] B.D. Aguda and R. Larter, J. Am. Chem. Soc. 112 (1990) 2167.

[11] H. Degn, Nature 217 (1968) 1047.